Supplementary Material of "INSERT TITLE" Submitted to *Royal Philosophical Transactions A*

Mehdi Ghazavi Dozein[a], Maldon Patrice Goodridge[b], Pierluigi Mancarella[a] and Andrea Pizzoferrato[c,d]

[a]The University of Melbourne, Melbourne VIC3010 AU
[b]Queen Mary University of London, London E14NS UK
[c]University of Bath, Bath BA27AY UK
[d]The Alan Turing Institute, London NW12DB UK

July 11, 2023

Contents

1 Automatic Voltage Regulation

The AVR scheme we use in the present work is summarized in Figure 1. Using as input value the voltage of the generic bus i, through a series of transformations, this protocol determines a voltage affecting the Rotor's field E_i which is gauged on a reference value. The AVR comprises of a Sensor, which measures the voltage through a potential transformer, an Amplifier, which magnifies the deviation w.r.t. a reference value, and an Exciter, which finally produces the potential impacting the generator. All these components are approximated by linear models. Usually, an AVR scheme also includes another transformation accounting for the Generator after the Exciter. However, this would imply a linearisation of the generator dynamical behaviour which would hide the level of detail in our non-linear description of the buses.

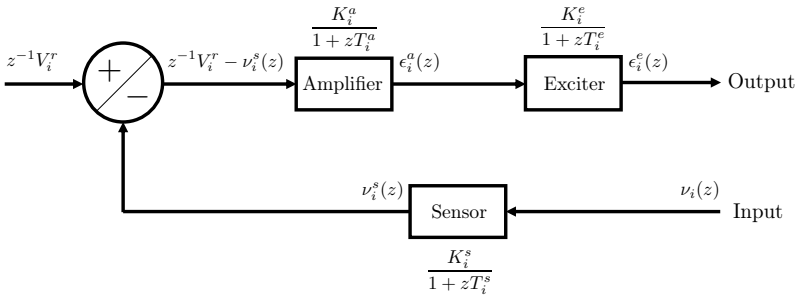

Figure 1: Diagram of the AVR scheme. The input voltage $\nu_i(t)$ is Laplace transformed and is then multiplied for the Sensor transfer function. The circle takes the difference between $\nu_i^s(t)$ and the reference value V^r (the z^{-1} prefactor is equal to 1 when inverse Laplace transformed, see (2b)). The result is used as the input of the Amplifier. The output value of the Exciter can be brought back to the time domain via the inverse Laplace transform. In the main text, we follow a different approach in which we inverse Laplace transform the action of each component of the diagram. The resulting input/output process is summarized in (2).

In the engineering literature [1], this sequence of transformations is usually expressed by means of transfer functions which describe the effect of each device in terms of its input/output Laplace transform. To avoid proliferation of notation, we indicate the Laplace transform of an observable by changing its argument label, for instance $\nu_i(z) = \mathcal{L}[\nu_i(t)](z)$ [1]. In this way, having in mind the components in Figure 1, the Sensor, Amplifier, and Exciter are defined as

$$\frac{\nu_i^s(z)}{\nu_i(z)} \coloneqq \frac{K_i^s}{1+zT_i^s}, \quad \frac{\epsilon_i^a(z)}{z^{-1}V_i^r - \nu_i^s(z)} \coloneqq \frac{K_i^a}{1+zT_i^a}, \quad \text{and} \quad \frac{\epsilon_i^e(z)}{\epsilon_i^a(z)} \coloneqq \frac{K_i^e}{1+zT_i^e}, \tag{1}$$

respectively, where the $K_i > 0$ are dimensionless quantities and the $T_i > 0$ are time constants. By bringing all the terms to the numerator, e.g. for the Sensor $\nu_i^s(z) + T_i^s z\nu_i^s(z) = K_i^s \nu_i(z)$, and then taking the inverse Laplace transform[2], we obtain the AVR scheme described in terms of a system of first-order differential equations

$$\begin{cases} \dot{\nu}_i^s(t) = \dfrac{1}{T_i^s}\left(K_i^s \nu_i(t) - \nu_i^s(t)\right) & \text{(2a)} \\ \dot{\epsilon}_i^a(t) = \dfrac{1}{T_i^a}\Big(K_i^a\left(V_i^r - \nu_i^s(t)\right) - \epsilon_i^a(t)\Big). & \text{(2b)} \\ \dot{\epsilon}_i^e(t) = \dfrac{1}{T_i^e}\left(K_i^e \epsilon_i^a(t) - \epsilon_i^e(t)\right) & \text{(2c)} \end{cases}$$

In practice, as the numerical solution of the power grid differential equation involves time discretisation, the output value of ϵ_i^e at time t is used for the evaluation of the voltage at the next time step, which generates a new ν_i to be fed in the AVR.

[1] As a quick reference for the Reader, we define the Laplace transform as $\mathcal{L}[f(t)](z) \coloneqq \int_{-\infty}^{\infty} f(t)e^{-zt}dt$ where z is a complex variable and $f(t)$ a time-varying function.

[2] The inverse Laplace transform is defined as $\mathcal{L}^{-1}[f(z)](t) \coloneqq \frac{1}{2\pi i}\lim_{T\to\infty}\int_{\gamma-iT}^{\gamma+iT} f(z)e^{zt}dz$. The usual assumptions hold that is the integration is done along the vertical line γ chosen to be greater than the real part of all singularities of $f(z)$ which is assumed to be bounded on this line.

2 Emergency Protection Schemes

In general, power grids can be subject to power disturbances, for instance as a consequence of the interaction with exogenous events or endogenous unexpected oscillations. We model these perturbations as instantaneous time-constant contributions to generator buses power load, that is

$$\eta(t) \coloneqq \underline{U}\Theta[t - t^*] \in \mathbb{R}^{N+L} \tag{3}$$

where $\underline{U}$ is the vector of disturbance magnitudes, Θ is the càdlàg Heaviside function and $t^* \gg 0$ is a time at which the system can be considered to be in its stationary state. In this paper, we consider disturbances applied on all the nodes but in general it is possible to specify a subset of the affected buses.

After a power disturbance occurs, emergency responses can be triggered when one or more of the observables values of the power grid buses exceed, within an observation time window $[0, T]$ with $T \in \mathbb{R}_+$ [s], their *Normal Operating Band* (NOB), which we describe, for a specific observable, as a closed interval (which we assume to be the same for every node in the network). Power grids reaction to frequency NOB violations consists in the activation of *emergency schemes* which, as typically implemented in industrial contexts, are mainly of two types: *Generation Shedding* (GS) and *Load Shedding* (LS). The former trips a generator device to arrest an increase in frequency or a general fluctuation in its RoCoF. The effect of GS is modelled by permanently setting to zero the power and Rotor's field on the failed node. The latter instead operates when frequency decreases from its stationary operational value by tripping customer loads. This effect can be taken into account by modelling LS protocol as power reduction on the load and, at the same time, decreasing the relevant dampening coefficient of the equivalent motor. As stated in the main paper, GS and LS are refereed in the engineering literature as *credible events*. We also model the *Line Tripping* (LT) emergency response, which belongs to the class known as *extreme events*, which works by disconnecting two nodes.

2.1 Generation Shedding

In more precise terms, we are interested in monitoring when the frequency deviation $\dot{\delta}(t) > F^+$ with $F^+ \in \mathbb{R}_+$. This can be achieved by considering the *over-frequency indicators*

$$\lambda_i^+(t) \coloneqq \Theta[\dot{\delta}_i(t) - F^+], \tag{4}$$

where, $i = 1, \ldots, N$. A similar approach can be used to control RoCoF variations [2]. Given a closed interval $[G^-, G^+]$ with $G^-, G^+ \in \mathbb{R}_+$ and $G^- < G^+$, the *RoCoF violation indicator* can be written as

$$\psi_i(t) \coloneqq \Theta[\ddot{\delta}_i(t) - G^+] + \Theta[G^- - \ddot{\delta}_i(t)], \tag{5}$$

During the observation time window, we can count the number of times the emergency schemes are activated in the power grid using the following *time-integrated counters* (whose definitions are motivated below)

$$\Lambda_i^+(t) \coloneqq \min\left\{1; \int_0^t \delta[1 + (\lambda_i^+(s_\varepsilon) - \lambda_i^+(s))]ds\right\}, \tag{6}$$

and

$$\Psi_i(t) \coloneqq \min\left\{1; \int_0^t \delta[1 + (\psi_i(s_\varepsilon) - \psi_i(s))]ds\right\}, \tag{7}$$

where $s_\varepsilon \coloneqq s - \varepsilon$ with $\varepsilon > 0$ arbitrarily small and, with little abuse of notation, here δ indicates Dirac delta function[3]. Finally, the GS emergency response resulting from over-frequency and RoCoF violation

[3]We assume that the integration domain is consistent with the chosen time discretisation and large enough to allow for the Dirac delta to be well defined, so that (6) and (7) are natural numbers

can be summarized as

$$\Xi_i \coloneqq (1 - \Theta[\Psi_i])(1 - \Theta[\Lambda_i^+]). \tag{8}$$

As can we see, once a GS is triggered on a node i we have $\Theta[\Psi_i]$ and/or $\Theta[\Lambda_i^+]$ equal to 1 which gives in turns $\Xi_i = 0$. The GS scheme does not remove the relevant node from the graph but only disconnect the generator from the network once a violation occurs (which motivates the min terms in (6) and (7)).

2.2 Load Shedding

To avoid outright blackouts, load is progressively shed as frequency decreases. This progression follows a step function, where each jump (activations of emergency response) corresponds to a different frequency. In formulas, given an ordered set of decreasing frequency deviation values $\underline{F}^- \coloneqq \{F_1^-, F_2^-, \dots, F_\Delta^-\}$ with $\Delta \in \mathbb{N}$ and $F_j^- < F^+$ for all j, we define a matrix $\hat{\lambda}^-$ of *under-frequency indicators* element-wise as

$$\lambda_{ij}^-(t) \coloneqq \Theta[F_j^- - \dot{\delta}_i(t)], \tag{9}$$

and the corresponding time-integrated counter matrix Λ^- as

$$\Lambda_{ij}^-(t) \coloneqq \min\left\{1; \int_0^t \delta[1 + (\lambda_{ij}^-(s_\varepsilon) - \lambda_{ij}^-(s))]ds\right\}, \tag{10}$$

where the first index runs over nodes $i = 1, \dots, N$ and the second over the under frequency set $j = 1, \dots, \Delta$. The proportion of load shed is then specified as

$$\Gamma_i(\Lambda^-) \coloneqq \sum_{j=1}^{\Delta} \Lambda_{ij}^- \in \{0, 1, \dots, \Delta\}. \tag{11}$$

This value affects the load via χ_i^L as explained in the main paper and the damping coefficient as (see [3] for a derivation of this formula, which results from noticing that the difference in total load before and after a single load shedding event is $C\Gamma_i P_i^L$)

$$D(\underline{\Gamma}) \coloneqq D\left[1 - \left(\frac{C}{\sum_{i=1}^{N+L} P_i^L}\right) \sum_{i=1}^{N+L} \Gamma_i P_i^L\right], \tag{12}$$

where nodes with no load shedding have the relevant $\Gamma_i = 0$.

2.3 Line Tripping

As characterized in the literature [4], the line connecting the loads i and j trips when two conditions are concurrently met. The first is verified when the power flowing through the line, which is defined as $\phi_{ij} \coloneqq B_{ij}\nu_i\nu_j \sin(\delta_i - \delta_j)$, exceeds a threshold value P^ϕ for the entire duration of a fixed time interval T^ϕ. So, following the same structure as for the preceding emergency responses, we define the *excess power flow indicator* as

$$\omega_{ij}(t) \coloneqq \Theta\left[\int_{t-T^\phi}^{t} \Theta[\phi_{ij}(s) - P^\phi]ds - T^\phi\right]. \tag{13}$$

The second controls if each bus frequency deviation exceeds a threshold $F^\phi < F^+$ during $[0, T^\phi]$. Similarly to (4), this results for the generic bus i in an over-frequency indicator and its corresponding time-integrated counter

$$\lambda_i^\phi \coloneqq \Theta[\dot{\delta}_i(t) - F^\phi], \quad \Lambda_i^\phi(t) \coloneqq \min\left\{1; \int_{t-T^\phi}^{t} \delta[1 + (\lambda_i^\phi(s_\varepsilon) - \lambda_i^\phi(s))]ds\right\}. \tag{14}$$

These conditions are combined in a single *line trip indicator* which reads as

$$\Omega_{ij}(t) \coloneqq 1 - \min\left\{1; \int_{T^{\phi}}^{t} \delta[\omega_{ij}(s)\Lambda_i^{\phi}(s)\Lambda_j^{\phi}(s) - 1]ds\right\}. \tag{15}$$

In the end, when a line tripping occurs between nodes i and j, the indicator Ω_{ij} switches from 1 to 0.

3 IEEE 39 Parameters

$$
B = \begin{bmatrix}
-42.1988 & 0 & 0 & 0 & 0 & 0 & 0 & 0 & 0 & 3.7656 & 0 & 0 & 0 & 0 & 0 & \dots \\
0 & -35.5333 & 2.1965 & 0 & 0 & 0 & 0 & 0 & 0 & 0 & 20.6982 & 0 & 7.4273 & 2.3492 & 0.7184 & \dots \\
0 & 2.1965 & -37.4811 & 0 & 0 & 0 & 0 & 0 & 0 & 0 & 16.4849 & 0 & 3.6444 & 8.7981 & 4.1052 & \dots \\
0 & 0 & 0 & -45.8275 & 0 & 0 & 0 & 0 & 0 & 0 & 0 & 0 & 0 & 0 & 0 & \dots \\
0 & 0 & 0 & 0 & -55.417 & 0 & 0 & 0 & 0 & 0 & 0 & 0 & 0 & 0 & 0 & \dots \\
0 & 0 & 0 & 0 & 0 & -50.6771 & 0 & 0 & 0 & 0 & 0 & 0 & 0 & 0 & 0 & \dots \\
0 & 0 & 0 & 0 & 0 & 0 & -36.7523 & 0 & 0 & 0 & 0 & 0 & 0 & 0 & 0 & \dots \\
0 & 0 & 0 & 0 & 0 & 0 & 0 & -43.0746 & 0 & 0 & 0 & 0 & 0 & 0 & 0 & \dots \\
0 & 0 & 0 & 0 & 0 & 0 & 0 & 0 & -63.9344 & 0 & 0 & 0 & 0 & 0 & 0 & \dots \\
3.7656 & 0 & 0 & 0 & 0 & 0 & 0 & 0 & 0 & -28.7041 & 0 & 0 & 16.4592 & 0 & 0 & \dots \\
0 & 20.6982 & 16.4849 & 0 & 0 & 0 & 0 & 0 & 0 & 0 & -168.9438 & 0 & 46.8403 & 17.6005 & 23.632 & \dots \\
0 & 0 & 0 & 0 & 0 & 0 & 0 & 0 & 0 & 0 & 0 & -215.7208 & 215.7598 & 0 & 0 & \dots \\
0 & 7.4273 & 3.6444 & 0 & 0 & 0 & 0 & 0 & 0 & 16.4592 & 46.8403 & 215.7598 & -293.7623 & 3.8895 & 1.1832 & \dots \\
0 & 2.3492 & 8.7981 & 0 & 0 & 0 & 0 & 0 & 0 & 0 & 17.6005 & 0 & 3.8895 & -35.9639 & 4.3813 & \dots \\
0 & 0.7184 & 4.1052 & 0 & 0 & 0 & 0 & 0 & 0 & 0 & 23.632 & 0 & 1.1832 & 4.3813 & -138.755 & \dots \\
0 & 0 & 0 & 18.9558 & 0 & 0 & 0 & 0 & 0 & 0 & 0 & 0 & 0 & 0 & 105.4166 & \dots \\
0 & 0 & 0 & 25.3661 & 54.9227 & 0 & 0 & 0 & 0 & 0 & 0 & 0 & 0 & 0 & 0 & \dots \\
0 & 0 & 0 & 0 & 0 & 20.1418 & 0 & 0 & 0 & 0 & 0 & 0 & 0 & 0 & 0 & \dots \\
0 & 0 & 0 & 0 & 0 & 29.3615 & 36.7523 & 0 & 0 & 0 & 0 & 0 & 0 & 0 & 0 & \dots \\
0 & 0 & 0 & 0 & 0 & 0 & 0 & 0 & 0 & 0 & 0 & 0 & 0 & 0 & 0 & \dots \\
21.2592 & 0 & 0 & 0 & 0 & 0 & 0 & 42.024 & 0 & 5.8459 & 0 & 0 & 0 & 0 & 0 & \dots \\
0 & 0 & 0 & 0 & 0 & 0 & 0 & 0 & 0 & 0 & 0 & 0 & 0 & 0 & 0 & \dots \\
0 & 0 & 0 & 0 & 0 & 0 & 0 & 0 & 0 & 0 & 0 & 0 & 0 & 0 & 0 & \dots \\
0 & 0 & 0 & 0 & 0 & 0 & 0 & 0 & 0 & 0 & 0 & 0 & 0 & 0 & 0 & \dots \\
0 & 0 & 0 & 0 & 0 & 0 & 0 & 0 & 62.375 & 0 & 0 & 0 & 0 & 0 & 0 & \dots \\
16.3457 & 0 & 0 & 0 & 0 & 0 & 0 & 0 & 0 & 4.6879 & 46.7741 & 0 & 0 & 0 & 0 & \dots \\
0 & 0 & 0 & 0 & 0 & 0 & 0 & 0 & 0 & 0 & 0 & 0 & 0 & 0 & 0 & \dots
\end{bmatrix}
$$

$$
\begin{bmatrix}
\dots & 0 & 0 & 0 & 0 & 0 & 21.2592 & 0 & 0 & 0 & 16.34 & 57 & 0 \\
\dots & 0 & 0 & 0 & 0 & 0 & 0 & 0 & 0 & 0 & 0 & 0 & 0 \\
\dots & 0 & 0 & 0 & 0 & 0 & 0 & 0 & 0 & 0 & 0 & 0 & 0 \\
\dots & 18.9558 & 25.3661 & 0 & 0 & 0 & 0 & 0 & 0 & 0 & 0 & 0 & 0 \\
\dots & 0 & 54.9227 & 0 & 0 & 0 & 0 & 0 & 0 & 0 & 0 & 0 & 0 \\
\dots & 0 & 0 & 20.1418 & 29.3615 & 0 & 0 & 0 & 0 & 0 & 0 & 0 & 0 \\
\dots & 0 & 0 & 0 & 36.7523 & 0 & 0 & 0 & 0 & 0 & 0 & 0 & 0 \\
\dots & 0 & 0 & 0 & 0 & 0 & 42.024 & 0 & 0 & 0 & 0 & 0 & 0 \\
\dots & 0 & 0 & 0 & 0 & 0 & 0 & 0 & 0 & 0 & 62.375 & 0 & 0 \\
\dots & 0 & 0 & 0 & 0 & 0 & 5.8459 & 0 & 0 & 0 & 0 & 4.6879 & 0 \\
\dots & 0 & 0 & 0 & 0 & 0 & 0 & 0 & 0 & 0 & 0 & 46.7741 & 0 \\
\dots & 0 & 0 & 0 & 0 & 0 & 0 & 0 & 0 & 0 & 0 & 0 & 0 \\
\dots & 0 & 0 & 0 & 0 & 0 & 0 & 0 & 0 & 0 & 0 & 0 & 0 \\
\dots & 0 & 0 & 0 & 0 & 0 & 0 & 0 & 0 & 0 & 0 & 0 & 0 \\
\dots & 105.4166 & 0 & 0 & 0 & 0 & 0 & 0 & 0 & 0 & 0 & 0 & 0 \\
\dots & -452.7209 & 19.6858 & 73.8149 & 0 & 169.0544 & 0 & 0 & 22.1387 & 0 & 0 & 0 & 46.6323 \\
\dots & 19.6858 & -100.3665 & 0 & 0 & 0 & 0 & 0 & 0 & 0 & 0 & 0 & 0 \\
\dots & 73.8149 & 0 & -123.7523 & 30.6077 & 0 & 0 & 0 & 0 & 0 & 0 & 0 & 0 \\
\dots & 0 & 0 & 30.6077 & -124.0966 & 28.459 & 0 & 0 & 0 & 0 & 0 & 0 & 0 \\
\dots & 169.0544 & 0 & 0 & 28.459 & -197.2989 & 0 & 0 & 0 & 0 & 0 & 0 & 0 \\
\dots & 0 & 0 & 0 & 0 & 0 & -122.6283 & 30.6588 & 0 & 0 & 0 & 25.0386 & 0 \\
\dots & 0 & 0 & 0 & 0 & 0 & 30.6588 & -133.5865 & 67.4157 & 20.9248 & 15.868 & 0 & 0 \\
\dots & 22.1387 & 0 & 0 & 0 & 0 & 0 & 67.4157 & -113.2189 & 0 & 0 & 0 & 24.0033 \\
\dots & 0 & 0 & 0 & 0 & 0 & 0 & 20.9248 & 0 & -86.071 & 65.6607 & 0 & 0 \\
\dots & 0 & 0 & 0 & 0 & 0 & 0 & 15.868 & 0 & 65.6607 & -141.7435 & 0 & 0 \\
\dots & 0 & 0 & 0 & 0 & 0 & 25.0386 & 0 & 0 & 0 & 0 & -166.5271 & 74.6771 \\
\dots & 46.6323 & 0 & 0 & 0 & 0 & 0 & 0 & 24.0033 & 0 & 0 & 74.6771 & -145.0171
\end{bmatrix}
$$

Sym.	Value	Values	Units
δ^0	Electrical Phase Angle (nodal; t = 0)	[0.9827 ,0.9879 ,0.9992 , 1.0072, 1.0039, 1.0143, 1.0236, 1.0044, 1.0238, 0.9529, 0.9578 0.9400, 0.9423, 0.9682, 0.9631 0.9690, 0.9849, 0.9779, 0.9941, 0.9694, 0.9780, 0.9724 0.9643, 0.9858, 0.9966, 0.9608, 0.9617]	[rad]
δ^0	Electrical Phase Angle (nodal; t = 0)	[0.9107, 0.9389, 0.9974, 1.0366, 1.0194, 1.0734, 1.1210, 1.0214, 1.1215, 0.7598, 0.7843, 0.6936, 0.7052, 0.8375, 0.8111, 0.8413, 0.9226, 0.8866, 0.9695, 0.8431, 0.8867, 0.8583, 0.8171 0.9264, 0.9818, 0.7994, 0.8042]	[rad]
δ^0	Electrical Phase Angle (nodal; t = 0)	[0.9294, 0.9513, 0.9975, 1.0291, 1.0156, 1.0581, 1.0959, 1.0173, 1.0965, 0.8094, 0.8289, 0.7569, 0.7661, 0.8711, 0.8502, 0.8743, 0.9387, 0.9102, 0.9759, 0.8757, 0.9103, 0.8877, 0.8550, 0.9419, 0.9859, 0.8409, 0.8447]	[rad]
δ^0	Electrical Phase Angle (nodal; t = 0)	[0.6598, 0.6965, 0.7519, 0.8355, 0.8282, 0.8862, 0.9860, 0.8393, 1.0002, 0.3871, 0.4451, 0.3008, 0.3185, 0.5225, 0.4898, 0.5383, 0.6710, 0.6060, 0.7371, 0.5409, 0.6213, 0.5787, 0.5105, 0.6928, 0.7808, 0.4767, 0.4843]	[rad]
$\dot{\delta}^0$	Rotor Angular Velocity (nodal; t = 0)	$[0, 0, \ldots, 0, 0] \in \mathbb{R}^{27} \forall \tau$	$[s^{-1}]$
$\ddot{\delta}^0$	Rate of Change of Frequency (nodal; t= 0)	$[0, 0, \ldots, 0, 0,] \in \mathbb{R}^{27} \forall \tau$	$[s^{-2}]$
v^0	Voltages (nodal; t= 0)	[0.9582, 0.9753, 0.9914, 0.9927, 0.9907, 0.9785, 1.0066, 0.9832, 0.9720, 0.9877, 0.9862, 0.9722, 0.9765, 0.9787, 0.9773, 0.9797, 0.9744, 0.9770, 0.9826, 0.9755, 0.9817, 0.9752, 0.9704 0.9722, 0.9784, 0.9754, 0.9715]	[p.u]
v^0	Voltages (nodal; t= 0)	[0.9531, 0.9657, 0.9793, 0.9829, 0.9834, 0.9672, 0.9959, 0.9751, 0.9601, 0.9830, 0.9762, 0.9655, 0.9685, 0.9718, 0.9697, 0.9710, 0.9655, 0.9665, 0.9698, 0.9670, 0.9736, 0.9685, 0.9650 0.9642, 0.9668, 0.9688, 0.9659]	[p.u]
v^0	Voltages (nodal; t= 0)	[0.9550, 0.9694, 0.9840, 0.9867, 0.9862, 0.9715, 1.0000, 0.9782, 0.9647, 0.9848, 0.9800, 0.9681, 0.9716, 0.9745, 0.9726, 0.9743, 0.9689, 0.9705, 0.9747, 0.9703, 0.9767, 0.9711, 0.9671 0.9672, 0.9712, 0.9714, 0.9680]	[p.u]
v^0	Voltages (nodal; t= 0)	[0.9558, 0.9534, 0.9653, 0.9698, 0.9722, 0.9523, 0.9790, 0.9629, 0.9591, 0.9760, 0.9629, 0.9563, 0.9576, 0.9633, 0.9596, 0.9592, 0.9526, 0.9522, 0.9511, 0.9553, 0.9624, 0.9597, 0.9578 0.9556, 0.9562, 0.9602, 0.9584]	[p.u]
P^0	Generator Power (nodal; t= 0)	[1.00, 1.908, 2.60, 2.528, 2.032, 2.60, 2.24, 2.16, 3.32, 4.00, 0, 0, . . . , 0, 0]	p.u
		[2.5, 4.771, 6.5, 6.32, 5.08, 6.5, 5.6, 5.4, 8.3, 10.0, 0, 0, . . . , 0, 0]	[p.u]
		[2.125, 4.0553, 5.525, 5.372, 4.318, 5.525, 4.76, 4.59, 7.055, 8.5, 0, 0, . . . , 0, 0]	[p.u]
		[3.25, 6.2023, 8.45, 8.216, 6.604, 8.45, 7.28, 7.02, 10.79, 13.0, 0, 0 . . . , 0, 0]	[p.u]
L^0	Loads (nodal; t= 0)	[0, 0.0368, 0, 0, 0, 0, 0, 0, 0, 0, 4.4160, 2.0000, 0.9352, 2.0880, 0.0300, 1.2800, 1.3160, 2.5120, 1.0960, 0.9900, 1.2344, 0.8960, 0.5560, 1.124, 0.8240, 1.1340, 1.2880, 0.6320]	[p.u]
		[0, 0.0920, 0, 0, 0, 0, 0, 0, 0, 0, 11.0400, 5.0000, 2.3380, 5.2200, 0.0750, 3.2000, 3.2900, 6.2800, 2.7400, 2.4750, 3.0860, 2.2400, 1.3900, 2.810, 2.0600, 2.8350, 3.2200, 1.5800]	[p.u]
		[0, 0.0782, 0, 0, 0, 0, 0, 0, 0, 0, 9.3840, 4.2500, 1.9873, 4.4370, 0.0638, 2.7200, 2.7965, 5.3380, 2.3290, 2.1038, 2.6231, 1.9040, 1.1815, 2.3885 1.7510, 2.4097, 2.7370, 1.3430]	[p.u]
		[0, 0.1196, 0, 0, 0, 0, 0, 0, 0, 0, 14.3520, 6.5000, 3.0394, 6.7860, 0.0975, 4.1600, 4.2770, 8.1640, 3.5620, 3.2175, 4.0118, 2.9120, 1.8070, 3.6530, 2.6780, 3.6855, 4.1860, 2.0540]	[p.u]
D	Load Damping Factor	2	[%]
T	Transient Time constant	[7.0000, 6.5600 , 5.7000 , 5.6900, 5.4000 , 7.3000 , 5.6600, 6.7000 , 4.7900 , 10.2000]	[s]
E_0	Rotor Field Voltage	0.95	[p.u]
	Governor Parameters		
A	Governor Droop Response	2	MW/Δf
g_d	Governor Dead-band Frequency Range	[59.95, 60.05]	[Hz]
	AVR Parameters		
T^s	Sensor Time Constant	0.05	[s]
K^s	Sensor Gain Constant	1	
T^a	Amplifier Time Constant	0.1	[s]
K^a	Amplifier Gain Constant	10	
T^e	Exciter Time Constant	1	[s]
K_e	Exciter Gain Constant	10	
	Protection Systems Parameters		
F^+	OFGS Threshold	62	[Hz]
T^{of}	OFGS Relay Delay	2	[s]
G^+, G^-	RoCoF Trip Threshold	-3, 3	$[Hzs^{-2}]$
T^{ro}	RoCoF Relay Delay	1	[s]
F^-	UFLS Threshold	{59.5, 59, 58.5, 58, 57.5}	[Hz]
T^{uf}	UFLS Relay Delay	2	[s]
P^ϕ	Line Trip Power Flow Deviation Threshold	510	[MW]
T^ϕ	Line Trip Relay Delay	4	[s]
	Two Area Generator Data		
P^{max}	Maximum Generator Power	[900, 900, 900, 900, 900, 900, 1000, 1000, 1500, 1500]	[MW]
H	Generator Inertia Constants	[5, 3.03, 3.58, 2.86, 4.33, 3.48, 2.64, 2.43, 3.45, 4.2]	[s]
X_d	Transient Reactance	4.05	[ohms]
X'_d	Sub-transient reactance	2.93	[ohms]
B	line susceptances	see below	[siemens]

Table 1: Table of parameters used in simulations conducted on the Two-Area Network.

Generator	Rating **(MVA)**	X_d **(pu)**	$X_d^{'}$ **(pu)**	$T_{d0}^{'}$ **(s)**	H **(s)**
G1	900	1.8	0.3	8	6.5
G1	900	1.8	0.3	8	6.5
G1	900	1.8	0.3	8	6.175
G1	900	1.8	0.3	8	6.175

Table 3: Generator Data for the Two-Area, Four Node Network: 900 MVA, 20kV base

From Bus	**To Bus**	**R (pu)**	**X (pu)**	**B (pu)**
1	5	0	0.15/9	0
2	6	0	0.15/9	0
3	11	0	0.15/9	0
4	10	0	0.15/9	0
5	6	25×0.0001	25×0.001	25×0.00175
10	11	25×0.0001	25×0.001	25×0.00175
6	7	10×0.0001	10×0.001	10×0.00175
9	10	10×0.0001	10×0.001	10×0.00175
7	8	110×0.0001	110×0.001	110×0.00175
7	8	110×0.0001	110×0.001	110×0.00175
8	9	110×0.0001	110×0.001	110×0.00175
8	9	110×0.0001	110×0.001	110×0.00175

Table 2: Transmission Network Data for the Two-Area, Four Node Network: 100 MVA, 230kV base. [3]

4 KTAS Parameters

The following susceptance matrices describe the reduce KTAS network before and after the line tripping. As explained in Section 2(a) of the main text, the susceptance matrix depends on the indicator function Ω which flips from 1 to 0 when a line tripping occurs. The difference occurs in line 5-6, which is the inter-connector line of the partially reduced network. So in the stationary regime we have

$$B(1) = \begin{bmatrix} -18.9278 & 7.8461 & 0 & 0 & 12.9499 & 0 \\ 7.8461 & -38.0413 & 0 & 0 & 32.5581 & 0 \\ 0 & 0 & -19.0178 & 7.8461 & 0 & 12.9499 \\ 0 & 0 & 7.8461 & -38.3713 & 0 & 32.5581 \\ 12.9499 & 32.5581 & 0 & 0 & -52.1891 & 9.0982 \\ 0 & 0 & 12.9499 & 32.5581 & 9.0982 & -50.6891 \end{bmatrix},$$

and after the line tripping

$$B(0) = \begin{bmatrix} -18.9278 & 7.8461 & 0 & 0 & 12.9499 & 0 \\ 7.8461 & -38.0413 & 0 & 0 & 32.5581 & 0 \\ 0 & 0 & -19.0178 & 7.8461 & 0 & 12.9499 \\ 0 & 0 & 7.8461 & -38.3713 & 0 & 32.5581 \\ 12.9499 & 32.5581 & 0 & 0 & -52.1891 & 0 \\ 0 & 0 & 12.9499 & 32.5581 & 0 & -50.6891 \end{bmatrix}.$$

Sym.	Value	Meaning	Units
δ^0	Electrical Phase Angle (nodal; t = 0)	$[0.4, 0.2, -0.1, -0.3, -0.1, -0.5]$	[rad]
$\dot{\delta}^0$	Rotor Angular Velocity (nodal; t = 0)	$[0, 0, 0, 0, 0, 0]$	$[s^{-1}]$
$\ddot{\delta}^0$	Rate of Change of Frequency (nodal; t= 0)	$[0, 0, 0, 0, 0, 0,]$	$[s^{-2}]$
v^0	Voltages (nodal; t= 0)	230	kV
P^0	Generator Power (nodal; t= 0)	$[735, 735, 735, 735, 0, 0]$	$[MW]$
L^0	Loads (nodal; t= 0)	$[100, 100, 50, 50, 967, 1, 767]$	MW
D	Load Damping Factor	2	[%]
T	Transient Time constant	8	[s]
E_0	Rotor Field Voltage	20	[kV]
Governor Parameters			
A	Governor Droop Response	2	MW/Δf
g_d	Governor Dead-band Frequency Range	$[59.95, 60.05]$	[Hz]
Battery Parameters			
B^m	Maximum Battery Power	$B^m \in \{0, 100, 200, ..., 1000\}$	MW
B^r	Maximum Battery Power for Regulation FCAS	$\frac{1}{2}B^m$	[MW]
B^0	Initial Battery State	bB^r where $b \sim \mathcal{U}[-0.01, 0.01]$	[MW]
T^b	AGC Signal Interval	4	s
T_0^b	Time Until the First AGC Signal	$T_0^b = tT^b$ where $t \sim \mathcal{U}[0, 1]$	[s]
B	Bias Factor	1.5	[MW/Δf]
F^D	Deadband Frequency Deviation	0.05	[Hz]
F^n	Emergency FCAS Frequency Deviation	0.15	[Hz]
F^m	Frequency deviation associated with Maximum Battery Power	1	[Hz]
AVR Parameters			
T^s	Sensor Time Constant	0.05	[s]
K^s	Sensor Gain Constant	1	
T^a	Amplifier Time Constant	0.1	[s]
K^a	Amplifier Gain Constant	10	
T^e	Exciter Time Constant	1	[s]
K_e	Exciter Gain Constant	10	
Protection Systems Parameters			
F^+	OFGS Threshold	62	[Hz]
T^{of}	OFGS Relay Delay	2	[s]
G^+, G^-	RoCoF Trip Threshold	-3, 3	$[Hzs^{-2}]$
T^{ro}	RoCoF Relay Delay	1	[s]
F^-	UFLS Threshold	$\{59.5, 59, 58.5, 58, 57.5\}$	[Hz]
T^{uf}	UFLS Relay Delay	2	[s]
P^{ϕ}	Line Trip Power Flow Deviation Threshold	510	[MW]
T^{ϕ}	Line Trip Relay Delay	4	[s]
Two Area Generator Data			
P^{max}	Maximum Generator Power	900	[MW]
H	Generator Inertia Constant	6.5,6.175	[s]
X_d	Transient Reactance	4.05	[ohms]
$X_d^{'}$	Sub-transient reactance	2.93	[ohms]
B	line susceptances	see below	[siemens]

Table 1: Table of parameters used in simulations conducted on the Two-Area Network.

Generator	Rating **(MVA)**	X_d **(pu)**	$X_d^{'}$ **(pu)**	$T_{d0}^{'}$ **(s)**	H **(s)**
G1	900	1.8	0.3	8	6.5
G1	900	1.8	0.3	8	6.5
G1	900	1.8	0.3	8	6.175
G1	900	1.8	0.3	8	6.175

Table 3: Generator Data for the Two-Area, Four Node Network: 900 MVA, 20kV base

From Bus	**To Bus**	**R (pu)**	**X (pu)**	**B (pu)**
1	5	0	0.15/9	0
2	6	0	0.15/9	0
3	11	0	0.15/9	0
4	10	0	0.15/9	0
5	6	25×0.0001	25×0.001	25×0.00175
10	11	25×0.0001	25×0.001	25×0.00175
6	7	10×0.0001	10×0.001	10×0.00175
9	10	10×0.0001	10×0.001	10×0.00175
7	8	110×0.0001	110×0.001	110×0.00175
7	8	110×0.0001	110×0.001	110×0.00175
8	9	110×0.0001	110×0.001	110×0.00175
8	9	110×0.0001	110×0.001	110×0.00175

Table 2: Transmission Network Data for the Two-Area, Four Node Network: 100 MVA, 230kV base. [3]

References

[1] K Eswaramma and G Surya Kalyan. An Automatic Voltage Regulator (AVR) system control using a P-I-DD controller. *International Journal of Advance Engineering and Research Development*, 4(6), 2017.

[2] AEMO. Fast Frequency Response in the NEM. https://www.aemo.com.au, 2017.

[3] Prabha Kundur, Neal J Balu, and Mark G Lauby. *Power system stability and control*, volume 7. McGraw-hill New York, 1994.

[4] M. G. Dozein and P. Mancarella. Possible negative interactions between fast frequency response from utility-scale battery storage and interconnector protection schemes. In *2019 29th Australasian Universities Power Engineering Conference (AUPEC)*, pages 1–6, 2019.